Kinematic Modeling of the Bárðarbunga Volcano Event

Hrvoje Tkalčić, *Lawrence Livermore National Laboratory, California, USA*
Douglas S. Dreger, *University of California at Berkeley, California, USA*
Gillian R. Foulger, *University of Durham, United Kingdom*
Bruce R. Julian, *United States Geological Survey, California, USA*

SUMMMARY:

Using the complete moment tensor time domain inversion method, we investigated the September 29, 1996 volcanic event of Mw=5.6 originated beneath the Bárðarbunga caldera in Iceland. The corresponding moment tensor is characterized by a significant non-double-couple component (NDC). The deviatoric inversion performed by using Iceland Hotspot Project IRIS-PASSCAL stations, yields a NDC solution with a 67% vertically oriented compensated linear vector dipole (CLVD) component, while the full moment tensor solution shows a similar, 66% CLVD component, 32% of double-couple component (DC) and a small volumetric contraction (ISO) of 2%. Statistical tests confirm that CLVD is a stable component of the moment tensor, while ISO is statistically insignificant.

Using an elastic finite difference code, with a large number of equidistantly distributed point sources we simulated various rupture scenarios on the walls of a conical surface of the Bárðarbunga caldera in order to compare them with the observations. Suites of seismograms for each independent run were produced at locations corresponding to HOTSPOT stations. We then inverted these synthetic data to investigate what portion of the original source information can be recovered by the moment tensor inversion. We were able to identify physical characteristics of a rupture scenario that produces synthetics which resemble the observed data to a quite high level of detail. We found that the rupture velocity, which took place at Bárðarbunga could have been a super-shear one, and we hypothesize that it could have been triggered by a compressional wave field that spread throughout the volume of the caldera.

Photo taken by Oddur Sigurdsson, IGS

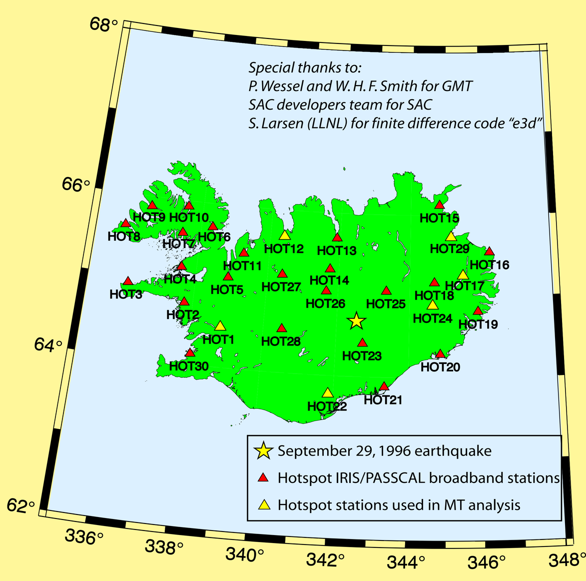

2. THE EARTHQUAKE AND IRIS-PASSCAL HOTSPOT STATIONS LOCATION

Map of Iceland showing the location of Iceland Hotspot IRIS-PASSCAL broadband stations (triangles) and the Sept. 29, 1996, earthquake (star) in the Bárðarbunga caldera. Although stations shown in yellow are used for the moment tensor inversion results shown in this poster, data from other stations are also analyzed and inverted for separately in order to put additional constraints on the moment. tensor solution. Note an excellent azimuthal coverage.

Deviatoric Solution (DC + CLVD)

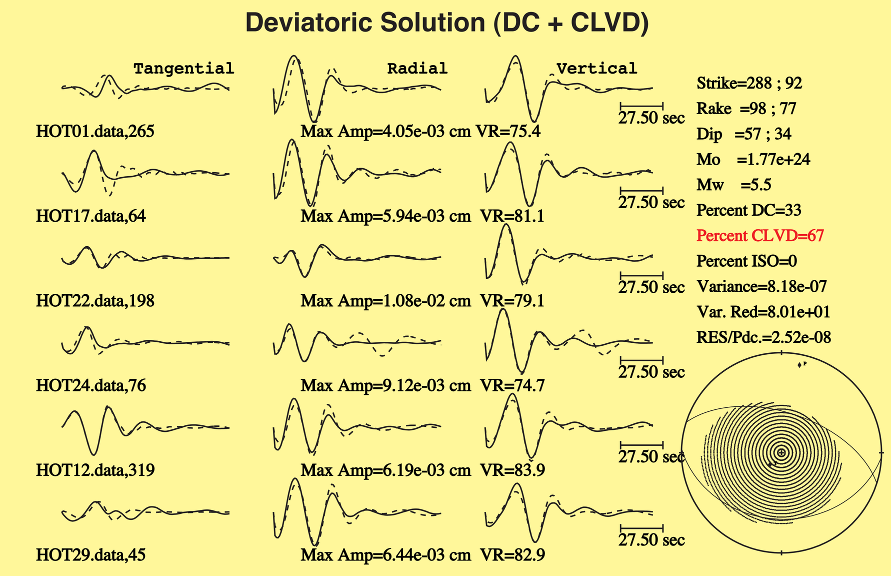

Full Moment Tensor Solution (DC + CLVD + ISO)

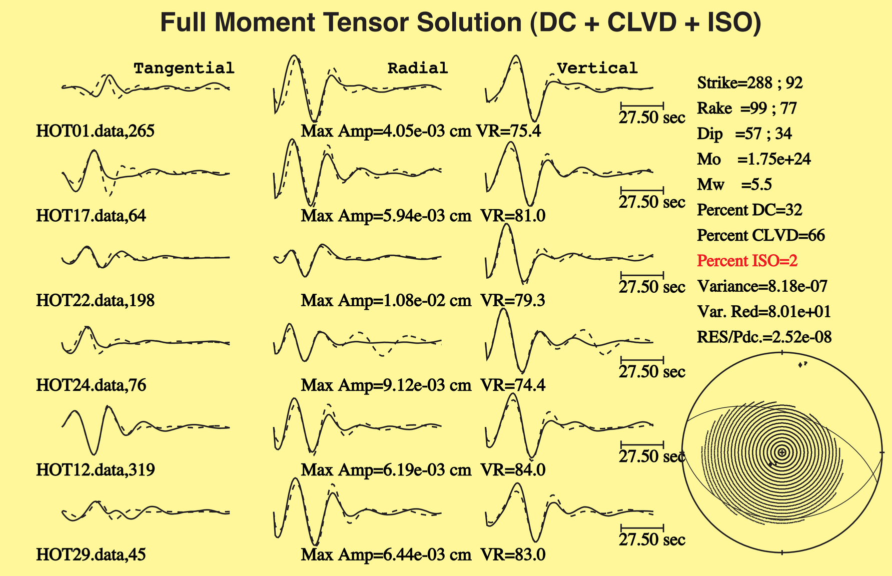

1. BACKGROUND:

On September 29, 1996, a sequence of earthquakes commenced, starting with a magnitude 5.6 earthquake in the Bárðarbunga caldera (Figure in upper right). Similar earthquakes had occurred in this area of Iceland previously. However this time the event was followed by a swarm of small earthquakes that extended to the neighboring volcanoes Grímsvötn and Hamarinn indicating widespread volcanic activation. The main event, a magnitude 5.6 earthquake, displayed an unusual pattern of seismic radiation, suggesting a mechanism that could not be explained with purely double-couple (DC) type of forces. A study of the event using teleseismic long-period and intermediate period surface wave data revealed solutions that are best described with a vertical compensated linear vector dipole (CLVD) and a mechanism in which a dominant vertically oriented vector dipole is in tension.

Following the earthquake, on September 30, an eruption broke out beneath the Vatnajokull glacier, SSW of the Bárðarbunga caldera, on the northern part of the Grímsvötn central volcano, and a large depression in the glacial ice was soon discovered from the air. This depression was explained as a consequence of an eruption on a 4km long NNE-SSW striking fissure beneath the glacier and glacier melting that took place after the eruption.

3. TIME DOMAIN MOMENT TENSOR INVERSION:

In order to invert for the moment tensor, we used a full waveform inversion described in previous work (2,3). Both deviatoric and full moment tensor solutions (FMT) were obtained for the Bárdarbunga earthquake (see figure on the right from the text). The FMT inversion allows for an isotropic process (explosion or collapse) and recovery of such a component is evidence for direct fluid involvement in the source process. The deviatoric inversion yielded an anomalous solution with a 67% CLVD component, while the FMT resulted in a similar, 66% CLVD component, accompanied by an insignificant volumetric contraction (ISO=2%). We performed a sensitivity test, in which we examined the stability of CLVD (presented by the value of epsilon) and isotropic components as a function of the number of stations used in the inversion. It can be seen that, as the number of the waveforms increases, CLVD component becomes very stable, reaching a value of about 0.35. On the other hand, isotropic component percentage decreases with increasing number of waveforms in the inversion.

Stability of CLVD and ISO: Jackknife Test

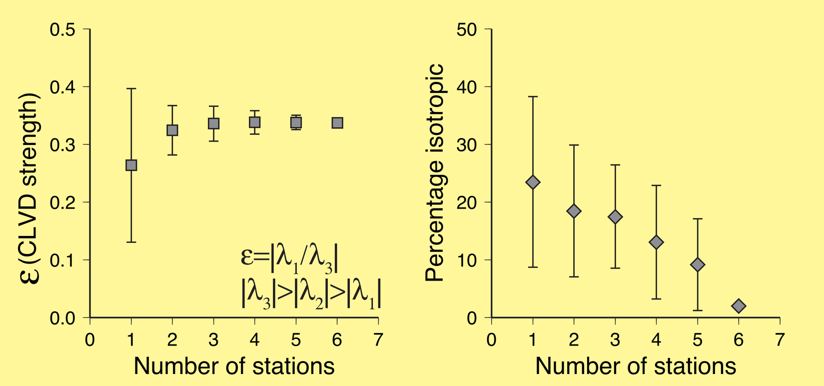

Full-Length Caldera Unilateral Rupture

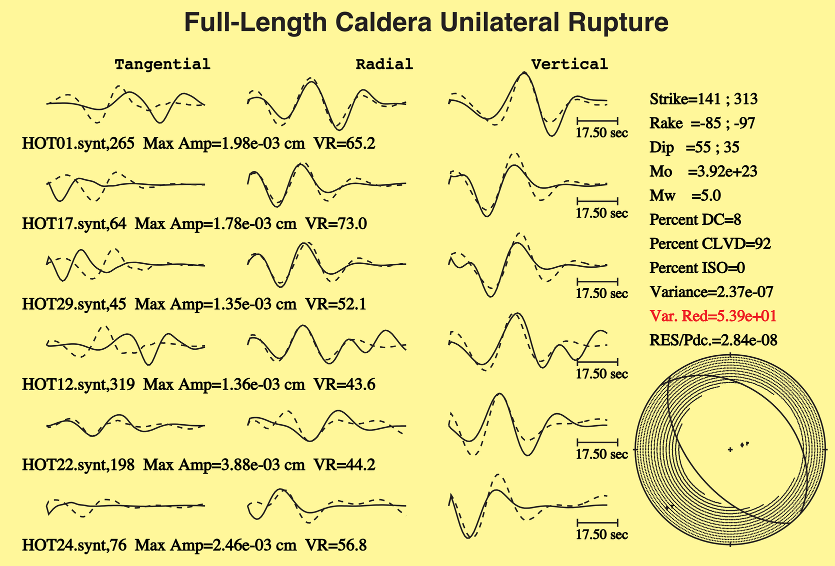

"Caldera Drop"

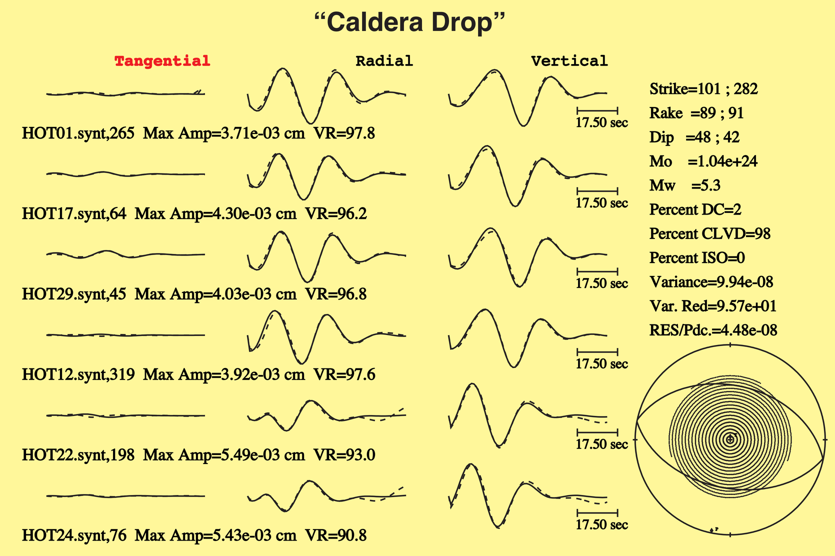

Quarter-Length Caldera Unilateral Rupture

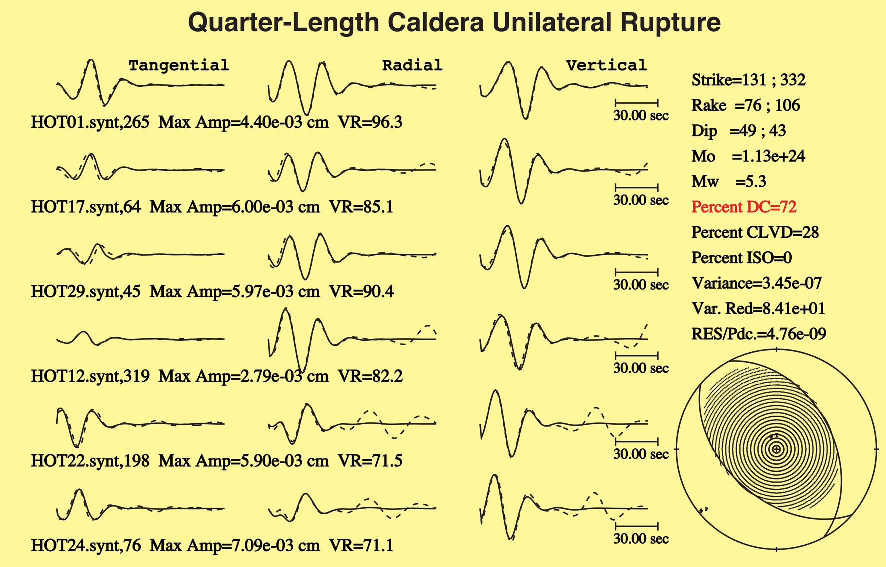

Full-Length Caldera Bilateral Rupture

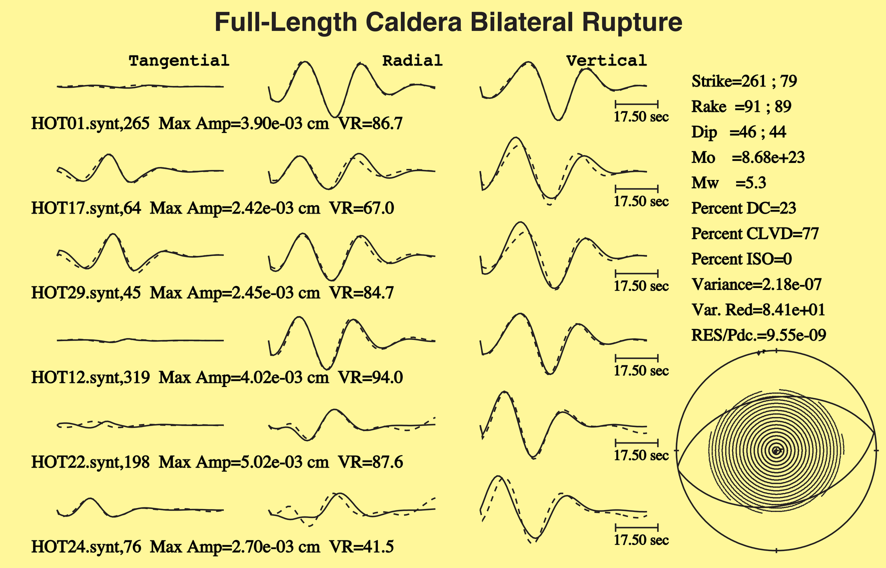

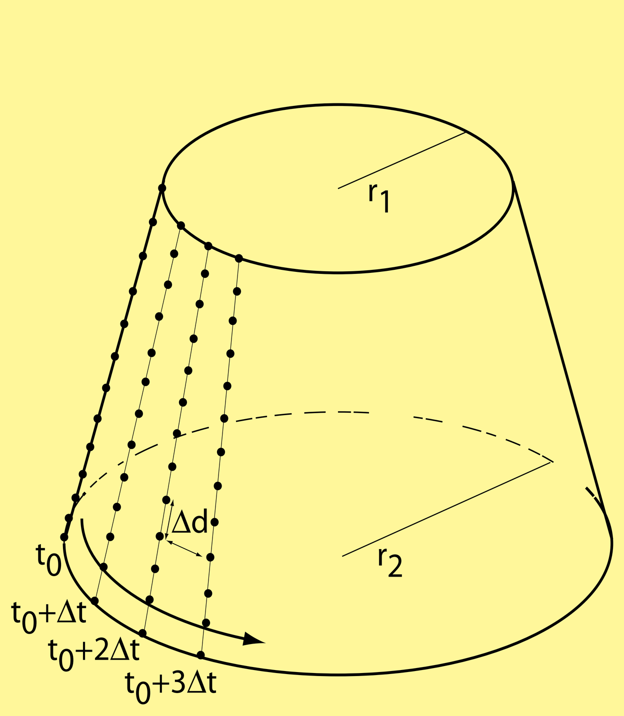

4. FINITE-SOURCE MODELING

We use a finite-difference code e3d (4) to generate synthetic waveforms from a 3D outward dipping caldera ring finite source models in a 1D-layered medium. In order to simulate the finite-source process multiple point sources equidistantly distributed over a conical surface, which resembles the surface of a caldera were used (see figure on the left). In this modeling we assumed uniform slip distribution and constant rupture velocity, although a range of rupture velocities from subshear to supershear was examined. We invert these synthetic data using time domain moment tensor inversion and the same station configuration (various scenarios of finite-source rupture are shown on the right-hand side of the text) .

6. FINITE-SOURCE SIMULATIONS RESULTS

Simulations were performed for full- (360°) half- (180°) and quarter-length (90°) unidirectional ruptures along the caldera walls initially assuming a Rayleigh wave speed of rupture (also shown is a bilateral model). The half-length rupture yields the variance reduction and orientation of the P axis similar to the observed. The full-length model does not fit as well as the half-length model because of the longer source duration. For the quarter-length model, the DC component dominates the solution, which is not consistent with the observation. "Simultaneous caldera drop" scenario does not produce tangential component of motion, which is not observed for the earthquake. We favor half-length rupture and bidirectional rupture models.

Half-Length Caldera Unilateral Rupture

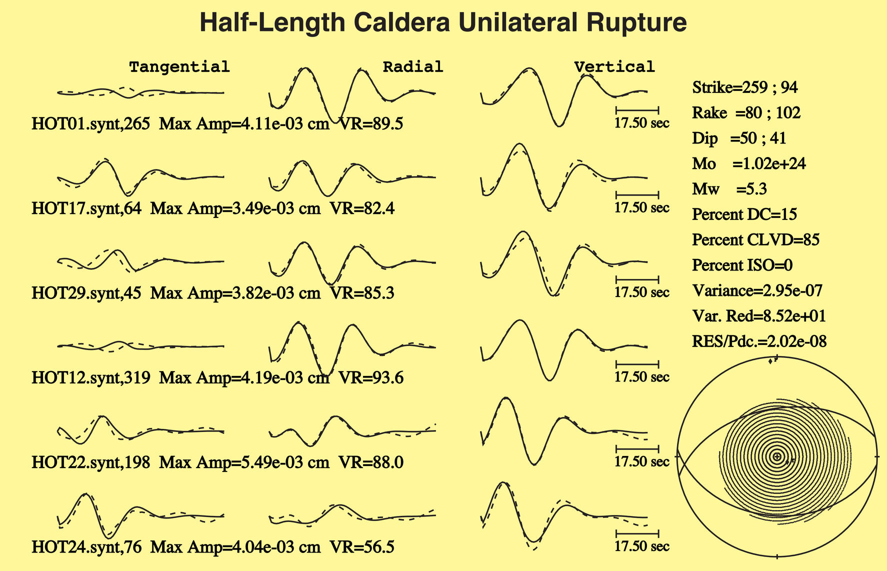

Variance Reduction from MT inversion assuming point source for the Green's functions and finite source e3d-synthetics for "data". A range of dipping angles and percentages of the caldera surface invoved in the rupture is tested in these simulations.

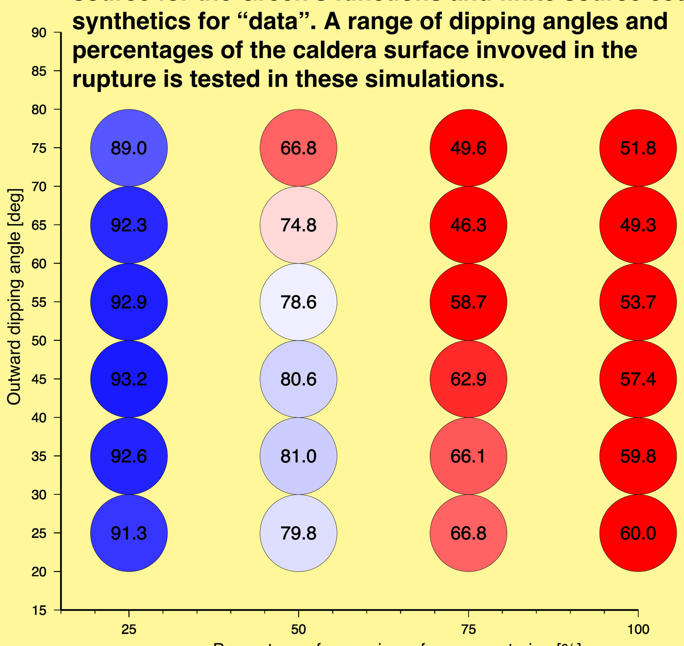

Starting point: 90° east of north on a circular fault
Synthetics from 6 stations are matched with Green's functions
Rupture speed = 3.1km/s
The dip. angle is the angle between the base of the cone and its wall

Focal mechanisms from MT inversion assuming point source for the Green's functions and finite source e3d-synthetics for "data". A range of dipping angles and percentages of the caldera surface invoved in the rupture is tested in these simulations.

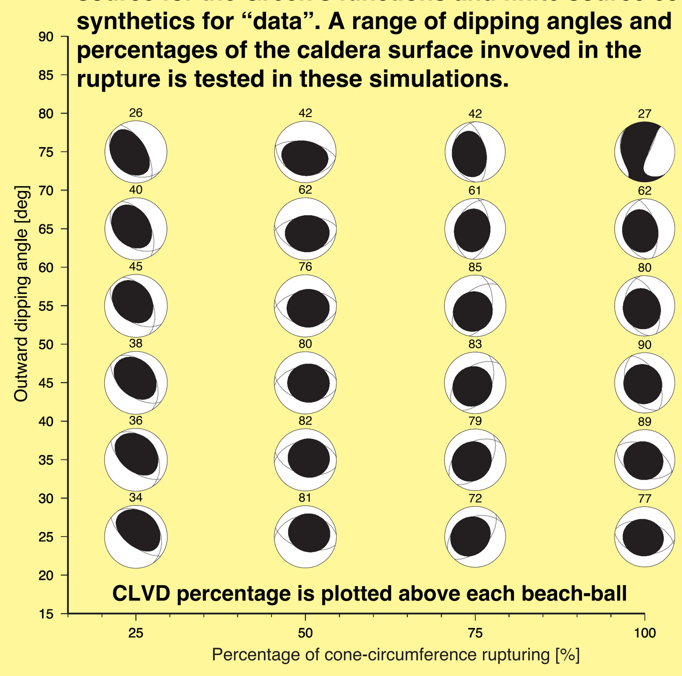

Starting point: 90° east of north on a circular fault
Synthetics from 6 stations are matched with Green's functions
Rupture speed = 3.1km/s
The dip. angle is the angle between the base of the cone and its wall

Variance Reduction and Wave Energy Variation With Rupture Speed

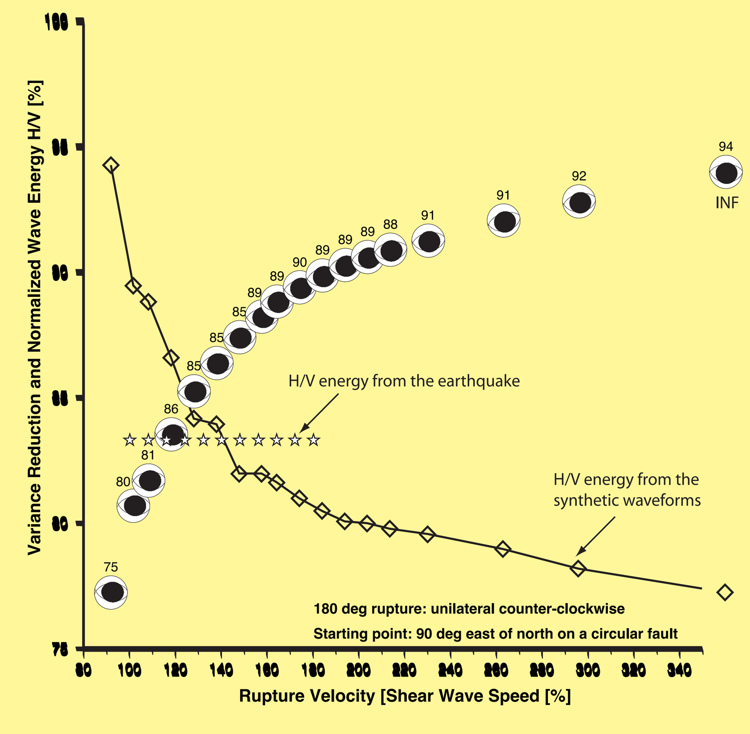

7. SUPER-SHEAR RUPTURE

We performed a series of finite-source simulations over a range of rupture velocity from subshear to supershear. We plot the obtained "beach-balls" at various speeds of rupture for the half-cone rupture scenario in the figure on the left. We also plot normalized ratios of horizontal- and vertical-component squared velocities (H/V energy) from the simulations and compare it with the observed H/V energy ratio. There is significant improvement in fit going from subshear to supershear rupture velocity. One physical mechanism for a supershear rupture velocity could be triggering of the rupture by the compressional wavefield that travels through the caldera.

5. TESTING FAULTING PARAMETERS

The finite-source simulations place bounds on faulting parameters in which it is possible to recover the observed moment tensor and simulate the observed seismic waveforms (see figures above). These results show that, while it is possible to achieve relatively high percentage of variance reduction (in waveform fit) with a quarter of the caldera rupturing (above right), the retrieved focal mechanisms are dominated by the double-couple component for all tested dipping angles of the caldera (above left). For larger portions of the caldera involved in the rupture process, the obtained CLVD component is still strong, however variance reduction is small in comparison to the observed variance reduction for the Bárðarbunga earthquake.

8. CONCLUSIONS:

The mechanism for the Bárðarbunga earthquake appears to be strongly NDC without a large isotropic component.

We modeled the observed Bárðarbunga earthquake mechanism with finite rupture processes on a conical surface.

Although our models are simplified in the sense of fault geometry, slip distribution (assumed uniform) and rupture velocity (assumed constant), they bracket the range of possible parameters in the finite-source process.

The modeling results indicate that in order to obtain the correct mechanism and waveforms consistent with the observations, super-shear rupture velocity is required.

An alternative model with two offset sources with similar but opposite volume changes cannot be ruled out as a viable explanation for the observed mechanism (5).

REFERENCES:

1. Nettles, M. and G. Ekström, *J. Geophys. Res.*, 103, 17973 (1998).
2. Dreger, D. S. and D. V. Helmberger, *J. Geophys. Res.* 98, 8107 (1993)
3. Dreger, D. S., H. Tkalčić and M. Johnston, *Science*, 288, 122 (2000)
4. Larsen, S. C. and D. B. Harris, *UCRL* (1993)
5. Julian, B. R., A. D. Miller and G. R. Foulger, *Rev. Geophys.*, 36, 525 (1998)